# HIGH RESOLUTION, MONOCHROMATIZED HeIIα EXCITED, PHOTOELECTRON SPECTRA OF $N_2$, CO AND $O_2$.

by

M. Carlsson Göthe, P. Baltzer, L. Karlsson,
B. Wannberg and S. Svensson.

Department of Physics,
Uppsala University,
Box 530, S-751 21 Uppsala,
Sweden

UUIP-1233 Oct. 1990

## Abstract

The valence photoelectron spectra of $N_2$, CO and $O_2$ excited using monochromatized HeIIα radiation are presented. Due to the high resolution and high signal-to-background ratio obtained in these spectra extensive new vibrational structure has been observed. New assignments of some of the photoelectron bands have been made to fit with the new features observed in the spectra. Vibrational progressions have in many cases been followed almost all the way up to the dissociation limits. Morse potential curves have been calculated for the states with clear vibrational progressions. Some potential curves show anomalous behavior such as double potential wells.

## INTRODUCTION

Numerous works have, using high resolution UV photoelectron spectroscopy (UPS), covered the outer valence regions of $N_2$, $O_2$ and CO. Most of these studies have been performed using HeIα resonance radiation, at 21.2 eV. However, in the study of the inner valence regions, higher excitation energies are needed than that supplied by the HeIα line. Studies have been carried out in UPS using HeIIα radiation (hν=40.8 eV), in X-ray photoelectron spectroscopy (XPS) using monochromatized Al Kα radiation (hν=1487 eV) and in photoelectron spectroscopy using tunable monochromatic synchrotron radiation (SRPS), with continuously variable wavelength. The width of the ionizing radiation obtained from gas discharges, such as HeI and HeII, is very small when proper conditions are used in the discharge. For example, our new ECR source [1] used in the present investigation produces intense HeIIα radiation which has a width (FWHM) of less than 4 meV when operated at normal pressures in the order of 50 mtorr. In such cases the instrumental contribution to the photoelectron linewidth is primarily determined by spectrometer function which is typically 10-50meV. However, these light sources produce both HeI and HeII radiation at different wavelengths. When recording HeIIα excited spectra, using unmonochromatized radiation from the discharge, an intense background appears, starting at about 26-28 eV. This background is due to excitations with the HeI radiation and makes studies of electronic states with higher binding energies impossible.

In a recent report we presented a new, focussing, monochromator for HeII radiation, which is used as a filter primarily to remove the HeI radiation [2]. By this monochromator the useful energy range in HeII photoelectron spectroscopy has been greatly extended. Furthermore, and equally important, the background in the photoelectron spectra is substantially reduced so that also weak structures can be studied in the inner valence region. In the present study monochromatized HeIIα radiation has been used in inner valence photoelectron spectroscopy of three small molecules; $O_2$, $N_2$ and CO. The spectra reveal several new states in the molecules. Furthermore, the vibrational structure appearing in some of the bands is well resolved.

The results of the present study give reason to reevaluate assignments performed in earlier studies of $N_2$, CO and $O_2$. In the cases of $N_2$ and CO, this has become necessary after comparing the new information obtained from the present HeIIα excited spectra with DES (resonance Auger) spectra of $N_2$ and CO by Eberhardt *et al* [3,4], and newly recorded XPS spectra of $N_2$ and CO [5].

## EXPERIMENT

The spectrometer used in the studies is an electron spectrometer dedicated to gas phase studies. The instrument has been described elsewhere [6]. The HeIIα radiation used in this study was produced using a high intensity 10GHz ECR source [1]. This light source has been used in a number of high resolution outer valence studies during the last year and is now commercially available. The HeIIα radiation from the discharge has been isolated by filtering out other radiation components using a newly designed monochromator [2]. The monochromator uses a toroidal grating with a ruling density of 800 l/mm which focuses the radiation into the gas cell.

The sample gas was obtained commercially with a purity of 99.995%. The gas pressure used was ≈ 20mTorr for all samples. No impurities were detected, except some helium leakage from the lamp. Due to this leakage, the He $1s_{1/2}$ line at 24.587 eV appears in all spectra. Since the energy of this line is very well determined it has been used for calibrating the spectra.

In order to determine the intensities and energies for the states observed in the present report a curve fitting method has been used that is described in ref. [7]. In the same report the computer aided tools used to construct the potential curves are outlined.

## RESULTS AND DISCUSSION

### The $N_2$ molecule

The $N_2$ photoelectron spectrum has previously been studied extensively. Outer valence spectra have recently been recorded in performance tests of the ECR lamp [1] using HeIIα and HeIIβ radiation. A high resolution HeII excited inner valence spectrum has been published by Åsbrink and Fridh [8].

The complete HeII excited spectrum obtained in the present study is shown in Fig. 1. The well-known outer valence photoelectron spectrum is seen between 15 and 20 eV. It corresponds to ionization from the three outermost orbitals in the valence electron configuration written as

$$2\sigma_g^2\, 2\sigma_u^2\, 1\pi_u^2\, 3\sigma_g^2$$

The $2\sigma_g$ orbital has a binding energy of approximately 38 eV and is not observed in the present spectrum. In the range between 20 and 35 eV a number of weak bands are observed, corresponding to the inner valence electron correlation states. The assignments of these in terms of the ionic states reached in the photoelectron transitions are given above each band. The interpretation of the spectrum has been discussed elsewhere [5] and is based on the results of the present spectrum, high resolution XPS, DES (resonance Auger) spectra and cal-

culations as mentioned above. A summary of the observed adiabatic and vertical energies for the bands seen in Fig. 1 is given in Table 1. In Table 2-4 we give the values for the vibrational levels of the X, A and B single hole states obtained in this study.

In Fig.2 we show a high resolution recording of the band observed at 25 eV. A strong progression can be observed which starts at 23.6 eV and is peaked at 25.5 eV. This progression fits well with the so called C state observed already by Gilmore [9]. The first peak at 23.6 eV coincides with the adiabatic energy given in this reference. Obviously, the progression can be followed up to v= 21, where the last three peaks are inferred on the low binding energy tail of the next band. The C- state dominates the XPS around 25 eV and corresponds to a $^2\Sigma^+_u$ state. This assignment is also confirmed by calculations [10-12]. The vibrational energies of the C state, observed in Fig. 2, are given in Table 5.

As was discussed in ref [5] the D $^2\Pi_g$ state is expected to appear on the low energy side of the band corresponding to the C state. Since it has $^2\Pi$ symmetry it has not been observed in the XPS. In the DES, however, a strong line can be seen at approximately 24.5 eV. In Fig. 2 we also discern a number of peaks around 24.5 eV that obviously belong to a weaker progression. This progression coincides with the D state given by Gilmore [9]. It should be noticed that this classification was later changed and in many reports the strong band around 29 eV has been referred to as the D state. In this report we use the notation of ref.[5]. Since this D band is superimposed on the stronger C band we cannot determine if the vibrational frequency corresponds to the visible peaks or if other peaks are hidden below the C band lines. Gilmores data indicate that the latter interpretation should be correct. The energies of the observed peak maxima in the D band are given in Table 6.

In ref.[5] it was shown that the E $^2\Pi_g$ state gives rise to the strong DES peak around 27.5 eV. The curve fitting in the region around 27.2 eV indicates the presence of a very weak progression, probably associated with this E $^2\Pi_g$ state. The vibrational energy cannot be unambiguously determined due to the superposition of lines associated with the C state. The region between 23 and 28 eV is therefore assigned in complete analogy with the corresponding region around 23.5 eV in the CO inner valence PES. The energies of the peak maxima of this E state are given in Table 7.

In Fig. 3 we show a detail of the spectrum in Fig. 2 ranging from 27-33.5 eV. The spectrum is dominated by a strong, essentially structureless peak centered around 28.8 eV. In ref. [5] this structure was explained as mainly due to the F $^2\Sigma^+_u$ state. On the high binding energy side of the XPS line in ref. [5] another weak component was observed which, by comparison to the DES spectrum, could be assigned to the G $^2\Pi_u$ state. In the present spectrum the structure around 30 eV observed in Fig. 3 can tentatively be interpreted in terms of two progressions, which may be associated with the G and H states which are expected in this energy region [5].

The I state is centred around 32 eV [5]. In Fig. 3 a number of clearly discernible vibrational lines can be seen in the low energy part of this band. Above 31.9 eV these lines are smeared out into a continuous distribution. The highest line seems to be somewhat broadened, *cf.*

Table 8. We therefore propose that this state is perturbed by a crossing with a dissociative potential curve at about 31.9 eV. A number of lines resulting from excitation with HeI stray-light are superimposed on the band. These lines makes it difficult to follow the extension of the band at higher binding energies. The intensity in the beginning of the band is very low. Due to the overlap with other bands it is therefore not possible to determine the adiabatic ionization energy.

## The CO molecule

The high resolution HeII excited photoelectron spectrum of CO has earlier been studied by Åsbrink *et al* [13] and by Potts and Williams [14]. In their spectra the inner valence region, starting with the D $^2\Pi$ state at 22.7 eV and the C $^2\Sigma^+$ state at 23.4 eV, shows extensive vibrational structure. However, the seventh state observed at 27-28 eV and assigned as F $^2\Sigma^+$ in ref. [13], is most uncertain due to an exponential HeI induced background.

In the present study, a new outer and inner valence photoelectron spectrum of CO has been recorded using monochromatized HeII$\alpha$ radiation. This spectrum, displayed in Fig. 4, shows nine resolved bands with binding energies below 33 eV. A summary of the vertical and adiabatic energies of the bands in Fig.4 is given in Table 9. The vibrational energies for the peaks in the well known X, A and B single hole states, as determined from the spectrum in Fig. 4, are given in Tables 10-12.

In the inner valence region above 20 eV the D $^2\Pi$ state is observed at 22.9 eV and the C $^2\Sigma^+$ state at 23.4 eV (vertical transitions). These observations correspond well to the results of refs [13,14]. It may be noted that the vertical ionization energy obtained from the well resolved XPS spectrum is 23.7 eV [5], which is 0.3 eV higher than the present result. Such a difference may arise if, for example, the electronic transition moment is not constant in the Franck-Condon region. The D- and C- states are obviously bound or quasi-bound with long vibrational progressions. A separate high resolution study of the interesting vibrational structure between 22 and 25 eV has recently been published [15]. The energies and intensities for the vibrational lines in the C and D states, as obtained from ref [15], are collected in Tables 13 and 14.

In Fig. 5 we show a detail of the spectrum in the energy region between 24 and 30 eV binding energy. In this region three states are observed; the E $^2\Pi$ state centred at 25.3 eV, the G $^2\Pi$ state centred at 27.4 eV and the F $^2\Sigma$ state centred at 28.2 eV (vertical ionization energies). The vibrational energies for the peaks in the E state, as determined from the spectrum in Fig. 5, is given in Tables 15. In the study of Åsbrink *et al*, the two bands at 27-28 eV and were not resolved and were therefore associated with transitions to a single state, referred to as the F $^2\Sigma^+$ state.

As may be seen in Fig. 5, the vibrational progression of the E state starts near the helium $1s_{1/2}$ line. It is therefore difficult to determine the adiabatic energy of the transition to the E state. We tentatively assign the peak at 24.755 eV to this transition. However, there may be unresolved components at even lower binding energies. Vibrational structure is observed in the entire region between 24.755 eV and the low binding energy tail of the F state. At about 26 eV, the vibrational progression seems to become irregular both in energy and intensity. This might suggest a crossing between different potential curves at approximately 26 eV. It should be noticed that the vibrational energies here assigned to the E state coincide with the predicted positions of the strong C state lines excited with 320 Å radiation. However, the relative intensities of these lines, compared to those of the C state, are almost two orders of magnitude higher than expected if they were due to this excitation, unless the cross section for the C state changes radically in this energy region (304 Å to 320 Å).

The band corresponding to the G state is essentially structureless, as is observed also in the case of $N_2$, although some weak features may be seen on the high binding energy side. The next clearly observed band, which we associate with the F state, is centred at about 28.1 eV. It shows a vibrational progression, which appears to start at 27.876 eV, *cf* Table 16. We tentatively associate this peak with the v=0 level although there may be weaker components hidden under the G band. As mentioned above, weak lines may be inferred superimposed on the high binding energy side of the G state and on the lines of the F state. This structure may be associated with the H state, which by comparison to the assignment for $N_2$, is expected to occur in this energy region.

The weak structure above 29 eV does not form a simple progression and the interpretation in this region will have to await more highly resolved studies. It might, however, be related to the I state which is expected to appear, with its maximum intensity, at about 31 eV [5]. A detailed recording of the energy region between 29 eV and 34 eV shown in Fig. 6 includes the range with both the I and J states. As can be seen, both states are essentially structureless with superimposed lines resulting from excitation of the X state with the HeI manifold. The almost triangular shape of the band supports the interpretation in terms of two states forming this band. It should be noticed that very weak structures are superimposed on the entire band. These structures may be due to indirectly populated vibrational levels in the X state [16,17] excited with the higher HeI components. this implies that the intermediate state is very broad, as was shown in ref [17]. At about 33 eV a progression of four lines is observed. These lines do not seem be due to be due to satellite lines in the UV radiation. They could therefore be related to the K state in $CO^+$. However, the vertical energy obtained from the XPS is 33.7 eV, which is 0.7 eV higher than the value of the UPS. The vibrational energies for the peaks in the state, as determined from the spectrum in Fig. 6, are given in Table 17. A peak is observed also at 31.88 eV. We have not found any explanation of this line in terms of other components present in the exciting radiation or any possible impurity in the sample gas. The peak is narrow and could correspond to a state in $CO^{+\cdot}$ An explanation of this line has to await further studies.

## The $O_2$ molecule

The high resolution HeI and HeII excited photoelectron spectrum of $O_2$ has earlier been studied by Edqvist *et al* [18]. The full spectrum obtained in the present study is shown in Fig. 7. A summary of the adiabatic and vertical ionization energies of the bands observed in this figure is given in Table 18.

The outer valence spectrum, including the X, a, A and b states, is similar to the corresponding spectrum given in ref. [18]. However, the signal to noise ratio is considerably higher in the present spectrum. Therefore, we observe many more lines than in previous studies. The detailed summary of the energies and relative intensities are given in Tables 19-22. It is interesting to note that the relative intensities differ markedly compared to those in ref [18] obtained using HeI radiation. This may reflect a variation in the electronic transition moment over the Franck-Condon region.

Fig. 8 shows a detail of the spectrum in the inner valence energy region between 20 and 29 eV binding energy with the B $^2\Sigma^-$, $^2\Pi$, c $^4\Sigma^-$ and $^2\Sigma^-$ states. The B state is found to have a long progression, observable up to v=16, *cf* Table 23. The latter of these vibrational components have relative intensities in the order of only 0.05% compared to the highest line in the band and have been possible to observe only due to the low background level.

The $^2\Pi$ state, centered around 23.9 eV, is found to be essentially structureless. On the high binding energy side of this band at least two very sharp lines are observed which reflect the transitions to the c $^4\Sigma^-$ state. Our identification of the lines is in line with that made in ref. [18]. According to Gilmore [9] the adiabatic energy of this state is 24.58 eV which is obscured by the helium $1s_{1/2}$ line at 24.587 eV. The c state is found to have a short vibrational progression. The vibrational energies and relative intensities are given in Table 24.

## POTENTIAL CURVES

The extensive vibrational structure observed in the photoelectron bands is useful for the determination of the potential curves of the cationic states. A series of calculations have been carried out for the observed cationic states in $N_2^+$, $CO^+$ and $O_2^+$ using Morse potential [20]. The potential curves for the neutral ground state have also been added. The equilibrium internuclear distances given by Huber and Herzberg [19] have been used for most of the curves. For the new states, not given in ref. [19] , the equilibrium bond distances have been obtained from a Franck-Condon analysis. These curves are presented in Fig 9-11.

## $N_2$

Detailed potential curves for $N_2$ and $N_2^+$ have been reported by Gilmore [9]. In the present study many more vibrational levels have been observed, for some of the states, than those used by Gilmore. It is therefore possible to determine the shape of the potential curves at higher energies than previously. Furthermore, vibrational structure has been observed for electronic states not included in Gilmores work. The potential curves for $N_2$, obtained in the present study, are shown in Fig. 9.

The potential curves for the three outer valence single hole states, in Fig. 9 have been calculated using the vibrational energies of the present study, and correspond well to those given by Gilmore [9]. Some peaks in the spectrum have been associated with high vibrational levels in the D state. These levels are entered into the potential curve obtained from ref. [9]. The transitions to the lower vibrational levels have not been observed due to an unfavorable Frank-Condon factor, *cf* Fig. 9. Since the vibrational levels of the state are observed above the dissociation energy limit at 24.3 eV, it must be assumed that the potential forms a barrier. Moreover, from the same observation it can be concluded that the potential curve must cross the Franck-Condon region in the range between 24 eV and 25 eV, as shown in the figure.

The C state progression has now been observed up to the v=21 level which allows a substantial extension of the potential curve, compared to that of refs. [8,9]. Obviously, the potential barrier inferred already by Gilmore is quite high and at least 1.1 eV. A plausible shape of the potential curve above the v=21 level has been indicated in Fig. 9. The vibrational levels of the E state are indicated in the left part of the figure. Since only a few levels are observed, it has not been possible to calculate a potential curve. However, it is clear that the shape of the curve forms a barrier similarly as for the C state since the dissociation energy limit is at 26.7 eV.

The structureless band associated with the F state is associated with a dissociative potential curve that crosses the Franck-Condon region in the range between 28 and 30 eV. This curve has been continued to the dissociation limit at 26.7 eV in the figure. As can be seen a crossing with the C state potential curve is predicted around v=15 for the latter curve. From Fig.2 a broadening of the lines around v=15 may well be inferred. The linewidths have been obtained in a curve fitting procedure, involving all the vibronic states and the general background in this range, giving an increase of the widths of approximately 20% when going from v= 13 to v=15. See Table 5.

The vibrational levels associated with the G and H states are marked in the diagram around 30 eV. No potential curve can be based on these energies. In Fig.3 it can be seen that the I state potential curve must cross the Franck-Condon region around 31.9 eV. The band starts with a discrete progression which shows a decreasing vibrational spacing with an increasing vibrational quantum number. Therefore, a potential minimum must exist. We have indicated a tentative curve in the top of Fig. 9. Since the structure is smeared out at about 31.9 eV a crossing repulsive potential curve may be inferred, as also is indicated in the figure.

## CO

Extensive studies of the valence potential curves of the ionic states of the CO molecule have previously been performed by Locht [21]. The potential curves derived in these studies were partly based on the observation of vibrational structure. In the present study we have observed several new vibrational states and are able to scetch the potential curves more accurately than in previous studies.

The X state has been studied in detail in refs. [16,17] using HeI and synchrotron radiation, respectively. These studies have permitted a detailed description of the potential curve up to v=33, which corresponds to an energy only approximately 1 eV below the dissociation limit. In ref.[17] it was pointed out that the extensive progression observed with excitation energies around 21-22 eV probably is due to a population of the vibrational states via an intermediate shape-resonant state. This model is supported by the results of the present study shown in Fig. 4. In the case of HeII excitation (hν=40.8 eV) only the direct Franck-Condon transitions are observed. This also implies that the intensities obtained from the present spectrum, given in Table 12, should better represent the Franck-Condon factors than the earlier HeI intensities which were affected by the two step population mechanism. It should be noticed that in the present spectrum both the v=1 and v=2 levels are observed and they have an intensity relative to the v=0 line that considerably deviates from the earlier, nonmonchromatized HeII results [22]. The intensities in Table 12 also agree very well with theoretical predictions of 4.2% and 0.2% for the v=1 and v=2 states, relative to the v=0 state, respectively [17]. These predictions were obtained using the intermolecular distance [19] and a Morse potential model. A potential curve for the X state is drawn in Fig. 10.

The energies and intensities for the A and B states agree well with earlier results [22]. The potential curves are shown in Fig.10.

An anomalous potential curve of the C state has earlier been predicted from a distorted vibrational energy distribution [23]. Locht [21] made the conclusion that this anomaly could be explained by a double minimum potential curve. In ref. [15] the vibrational structure is well resolved and allows a detailed description of the potential curve from the region around the potential minimum out to the dissociation limit. The curve corresponds to a double potential well where the vibrational states fall in two distinct essentially harmonic progressions, below and above the perturbation. This perturbation occurs at an internuclear distance of about 1.4 Å. The vibrational progression continues at least 0.2 eV above the dissociation limit for the $CO^+ \rightarrow C^+(^2P) + O(^1D)$ process at 24.19 eV. This implies another perturbation leading to a potential barrier around 2.3 Å internuclear distance, cf Fig 10.

As in the case of $N_2$ the D state is observed at lower binding energies than the C state. However, in the CO spectrum the vibrational structure of the D state is much more clearly observed than for $N_2$. The vibrational energies and intensities of the levels up to v=6 have been determined and are collected in Table 16. Since there is an overlap between the lines of the D band with the lines of the B state excited by the 320 Å line from the He discharge it is not obvious which line should be identified with the 0-0 transition to the D state. As dis-

cussed in ref. [12] the adiabatic binding energy can be associated with the line at 22.2 eV. Using these data a Franck-Condon analysis has been performed. From this analysis the equilibrium bond distance has been found to be 1.34 Å. The Morse potential curve which has been fitted to the observed vibrational levels is shown in Fig. 10.

The E state exhibits a rather long vibrational progression. However, as discussed above, the adiabatic ionization energy is not easily obtained since the beginning of the band is obscured by both the helium line at 24.587 eV and the high energy tail of the C state. Therefore it is not possible to derive unambiguously the potential curve of this state. The potential curve shown in Fig 11 obtained has been calculated using the assumption that the first observed peak at 24.755 eV corresponds to the adiabatic transition. As discussed above there may be a curve crossing at about 26.1 eV as suggested by the irregular vibrational structure in this energy region. The crossing potential curve is probably associated with the dissociative G $^2\Pi$ state. The vibrational structure above the crossing point is tentatively indicated by the dashed lines in Fig. 5.

Around 28 eV we clearly observe a vibrational progression that can be associated with the F $^2\Sigma^+$ state. The potential curve constructed from our data, which is indicated in Fig. 10.

The progression around 33 eV which is tentatively associated with the K state is clearly discernible and the adiabatic energy is readily obtained. The corresponding potential curve is included in Fig.10.

## $O_2$

In Fig. 11 we display the Morse potential curves obtained in a Franck-Condon analysis of the observed vibrational structure. Most curves agree with those given by Gilmore [9]. However, the B $^2\Sigma_g^-$ state has not been accurately determined in previous investigations since only a few vibrational levels have been observed. In the present work the progression may be followed up to v=16 which lies at 21.910 eV. This value is only 50 meV from the dissociation limit. The fit of the Morse curve shows, however, that a small potential barrier may exist, as indicated in Fig. 11.

The $^2\Pi_u$ state corresponds to a symmetric and structureless line around 23.9 eV. This indicates that the associated potential curve is dissociative. The c $^4\Sigma_u^-$ state is schematically drawn in Fig. 11. The next state has $^2\Sigma_u^-$ symmetry and the corresponding structureless symmetric line indicates a repulsive potential curve around 27.3 eV in the Franck-Condon region.

## CONCLUSIONS

The use of monochromatized HeIIα excitation of photoelectron spectra has enabled a much more detailed study of the inner valence region of $N_2$, CO and $O_2$ than has hitherto been possible. A large number of new features have been identified in the spectra and for some of the states the vibrational progressions have been followed to much higher quantum numbers than in previous studies. Using these vibrational energies and intensities it has been possible to calculate the Morse potential curves for the observed electronic states. Some of the curves show interesting behavior such as double potential wells. Future investigations using monochromatized HeII radiation in conjunction with improved spectrometer resolution will enable even more detailed studies and will give important clues to the interesting correlation phenomena in the inner valence region of molecules.

## REFERENCES


[1] P. Baltzer and L. Karlsson, Uppsala University Institute of Physics Report, UUIP-1211, 1989.

[2] P. Baltzer, M. Carlsson-Göthe, B. Wannberg and L. Karlsson, Uppsala University Institute of Physics Report, UUIP-1228, 1990.

[3] W. Eberhardt, E. W. Plummer, C. T. Chen and D. K. Ford, Austr. J. Phys., 39, 853 (1986).

[4] W. Eberhardt, E. W. Plummer, I. -W. Lyo, R. Murphy, R. Carr and W. K. Ford, J. Phys. (Paris) Colloque C9, Suppl. 12, 697 (1987).

[5] S. Svensson, M. Carlsson Göthe, A. Nilsson, L. Karlsson, N. Mårtensson and U. Gelius, Uppsala University Institute of Physics Report, UUIP-1200, 1990 and subm. for publ. in Chem. Phys. 1990.

[6] Peter Baltzer, Björn Wannberg and Mats Carlsson Göthe, Acc. for publ. in Rev. Sci. Instr., 1990.

[7] M. Carlsson-Göthe, L.Karlsson, S.Svensson and J. de Sousa Pires. Uppsala University Institute of Physics Report, UUIP-1237, 1990 and subm. to Computers in Physics, 1990.

[8] L. Åsbrink and C. Fridh, Physica Scripta. 9, 338-340, 1974.

[9] F. R. Gilmore, Mem. RM-4034-PR, The RAND Corp., 1964.

[10] H. Ågren, R. Arneberg, J. Müller and R. Manne, Chem. Phys., 83, 53 (1984).

[11] J. Schirmer and O. Walter, Chem. Phys. 78, 201 (1983).

[12] M. Okuda and N. Jonathan, J. Electron Spectrosc. 3, 19 (1974).

[13] L. Åsbrink, C. Fridh, E. Lindholm and K. Codling, Phys. Scr.10, 183 (1974).

[14] A. W. Potts and T. A. Williams, J. Electron Spectrosc., 3, 3 (1974).

[15] M. Carlsson-Göthe, B. Wannberg, L. Karlsson, S.Svensson and P. Baltzer, Uppsala University Institute of Physics Report, UUIP-1236, 1990.

[16] B. Wannberg, D. Nordfors, K. L. Tan, L. Karlsson and L. Mattson, J. Electron Spectrosc., 47, 147 (1988).

[17] L. Karlsson, S. Svensson and A. Svensson, J. Phys. B, 22, 3423 (1989).

[18] O. Edqvist, E. Lindholm, L. E. Selin and L. Åsbrink, Phys. Scr. 1, 25 (1970).

[19] K. P. Huber and G. Herzberg, *Molecular Spectra and Molecular Structure IV. Constants of diatomic molecules*. Van Nostrand Reinhold, NY 1979.

[20] G. Herzberg, *Molecular Spectra and Molecular Structure I. Spectra of diatomic molecules*. Van Nostrand Reinhold, NY, 1950.

[21] R. Locht, Chem. Phys. 22, 13 (1977).

[22] J. L. Gardner and J. A. R. Samson, J. Electron Spectrosc. 13, 7 (1978).

[23] K. Codling and A. W. Potts, J. Phys. B, 7, 163 (1974).

## TABLES

*Table 1. Summary of the observed states in $N_2^+$.*

| State Designation [a] | Adiabatic Ionization Energy (eV) | Vertical Ionization Energy (eV) |
|---|---|---|
| $X\ ^2\Sigma_g^+$ | 15.582 | 15.582 |
| $A\ ^2\Pi_u$ | 16.693 | 16.926 |
| $B\ ^2\Sigma_u^+$ | 18.775 | 18.775 |
| $C\ ^2\Sigma_u^+$ | 23.583 | 25.513 |
| $D\ ^2\Pi_g$ | 23.964 | 24.696 |
| $E\ ^2\Pi_g$ | 27.05 | 27.05 |
| $F\ ^2\Sigma_g^+$ | - | 28.8 |
| $G\ ^2\Pi_u$ | - | 30.2 |
| $H\ ^2\Pi_u$ | - | 30.2 |
| $I\ ^2\Sigma_u^+$ | - | 32 |

a This classification differs from previous UPS works.

*Table 2. Vibrational energy levels for the $X^2\Sigma_g^+$ state in $N_2^+$.*

| Vibrational quantum number. v | Binding Energy (eV) | Line Width (FWHM) (eV) | Relative Intensity |
|---|---|---|---|
| 0 | 15.582 | 0.075 | 1.000 |
| 1 | 15.851 | 0.075 | 0.098 |
| 2 | 16.116 | 0.073 | 0.014 |
| 3 | 16.375 | 0.064 | 0.002 |

*Table 3. Vibrational energy levels for the $A^2\Pi_u$ state in $N_2^+$.*

| Vibrational quantum number. v | Binding Energy (eV) | Line Width (FWHM) (eV) | Relative Intensity |
|---|---|---|---|
| 0 | 16.693 | 0.071 | 0.80 |
| 1 | 16.926 | 0.075 | 1.00 |
| 2 | 17.153 | 0.075 | 0.68 |
| 3 | 17.376 | 0.071 | 0.35 |
| 4 | 17.599 | 0.075 | 0.15 |
| 5 | 17.816 | 0.075 | 0.059 |
| 6 | 18.029 | 0.073 | 0.021 |
| 7 | 18.240 | 0.075 | 0.008 |
| 8 | 18.449 | 0.075 | 0.003 |

*Table 4. Vibrational energy levels for the $B^2\Sigma_u^+$ state in $N_2^+$.*

| Vibrational quantum number. v | Binding Energy (eV) | Line Width (FWHM) (eV) | Relative Intensity |
|---|---|---|---|
| 0 | 18.755 | 0.073 | 1.00 |
| 1 | 19.044 | 0.071 | 0.12 |
| 2 | 19.259 | 0.073 | 0.008 |
| 3 | 19.475 | 0.075 | 0.005 |
| 4 | 19.706 | 0.075 | 0.002 |
| 5 | 19.917 | 0.099 | 0.0009 |
| 6 | 20.112 | 0.120 | 0.0004 |
| 7 | 20.307 | 0.071 | 0.0002 |

*Table 5. Vibrational energy levels for the $C^2\Sigma_u^+$ state in $N_2^+$.*

| Vibrational quantum number. v | Binding Energy (eV) | Line Width (FWHM) (eV) | Relative Intensity |
|---|---|---|---|
| 0 | 23.583 | 0.094 | 0.024 |
| 1 | 23.833 | 0.094 | 0.13 |
| 2 | 24.086 | 0.092 | 0.34 |
| 3 | 24.332 | 0.099 | 0.57 |
| 4 | 24.577 [a] | | |
| 5 | 24.816 | 0.094 | 0.86 |
| 6 | 25.052 | 0.082 | 0.96 |
| 7 | 25.285 | 0.085 | 0.99 |
| 8 | 25.513 | 0.082 | 1.00 |
| 9 | 25.735 | 0.080 | 0.94 |
| 10 | 25.954 | 0.082 | 0.80 |
| 11 | 26.168 | 0.082 | 0.66 |
| 12 | 26.376 | 0.080 | 0.50 |
| 13 | 26.577 | 0.089 | 0.40 |
| 14 | 26.771 | 0.094 | 0.31 |
| 15 | 26.960 | 0.113 | 0.24 |
| 16 | 27.147 | 0.125 | 0.22 |
| 17 | 27.319 | 0.127 | 0.15 |
| 18 | 27.478 | | |
| 19 | 27.602 | | |
| 20 | 27.715 | | |
| 21 | 27.819 | | |

a Obscured by impurity line.

*Table 6. Vibrational energy levels for the $D^2\Pi_g$ state in $N_2^+$.*

| Vibrational quantum number. v | Binding Energy (eV) | Line Width (FWHM) (eV) | Relative Intensity |
|---|---|---|---|
| a | 23.964 | 0.10 | 0.34 |
| | 24.202 | 0.09 | 0.66 |
| | 24.459 | 0.09 | 0.93 |
| | 24.696 | 0.09 | 1.00 |
| | 24.940 | 0.09 | 0.78 |
| | 25.168 | 0.09 | 0.66 |
| | 25.396 | 0.09 | 0.55 |

a Uncertain vibrational quantum number designation.

*Table 7. Vibrational energy levels for the $E^2\Pi_g$ state in $N_2^+$.*

| Vibrational quantum number. v | Binding Energy (eV) | Line Width (FWHM) (eV) | Relative Intensity |
|---|---|---|---|
| a | 27.052 | 0.07 | 1.00 |
| | 27.239 | 0.06 | 0.53 |
| | 27.400 | 0.05 | 0.32 |
| | 27.542 | 0.05 | 0.21 |
| | 27.670 | | |

a Uncertain vibrational quantum number designation.

*Table 8. Vibrational energy levels for the $I^2\Pi_u^+$ state in $N_2^+$.*

| Vibrational quantum number. v | Binding Energy (eV) | Line Width (FWHM) (eV) | Relative Intensity |
|---|---|---|---|
| a | 30.815 | 0.12 | 0.2 |
| | 31.010 | 0.11 | 0.4 |
| | 31.200 | 0.10 | 0.6 |
| | 31.375 | 0.09 | 1.0 |
| | 31.545 | 0.09 | 0.8 |
| | 31.713 | 0.11 | 0.4 |

a Uncertain vibrational quantum number designation.

*Table 9. Summary of the observed states in $CO^+$.*

| State Designation | Adiabatic Ionization Energy (eV) | Vertical Ionization Energy (eV) |
|---|---|---|
| $X\ ^2\Sigma$ | 14,018 | 14,018 |
| $A\ ^2\Pi$ | 16,456 | 16,917 |
| $B\ ^2\Sigma^+$ | 19,671 | 19,671 |
| $C\ ^2\Sigma^+$ | 23,01 | 23,381 |
| $D\ ^2\Pi$ | 22,204 | 22,726 |
| $E\ ^2\Pi$ | 24,755 | 25,294 |
| $G\ ^2\Pi$ | - | 27,36 |
| $F\ ^2\Sigma^+$ | 27,876 | 28,240 |
| H | - | 28.0 |
| $I\ ^2\Sigma^+$ | - | 31,14 [a] |
| $J\ ^2\Sigma^+$ | - | 31,95 [a] |
| $K\ ^2\Sigma^+$ | 32,814 | 32,984 |

[a] Value given by Svensson *et al* [5] from XPS.

*Table 10. Vibrational energy levels for the $X^2\Sigma$ state in $CO^+$.*

| Vibrational quantum number, v | Binding Energy (eV) | Line Width (FWHM) (eV) | Relative Intensity |
|---|---|---|---|
| 0 | 14,018 | 0,068 | 1,000 |
| 1 | 14,288 | 0,068 | 0,045 |
| 2 | 14,554 | 0,118 | 0,001 |

*Table 11. Vibrational energy levels for the $A^2\Pi$ state in $CO^+$.*

| Vibrational quantum number, v | Binding Energy (eV) | Line Width (FWHM) (eV) | Relative Intensity |
|---|---|---|---|
| 0 | 16,456 | 0,068 | 0,41 |
| 1 | 16,730 | 0,068 | 0,81 |
| 2 | 16,917 | 0,068 | 1,00 |
| 3 | 17,100 | 0,068 | 0,89 |
| 4 | 17,280 | 0,068 | 0,64 |
| 5 | 17,456 | 0,068 | 0,41 |
| 6 | 17,630 | 0,068 | 0,23 |
| 7 | 17,800 | 0,068 | 0,12 |
| 8 | 17,966 | 0,071 | 0,06 |

*Table 11. Continued.*

| | | | |
|---|---|---|---|
| 9 | 18,131 | 0,071 | 0,03 |
| 10 | 18,292 | 0,071 | 0,02 |
| 11 | 18,449 | 0,073 | 0,007 |
| 12 | 18,612 | 0,085 | 0,004 |
| 13 | 18,749 | 0,071 | 0,003 |

*Table 12. Vibrational energy levels for the $B^2\Sigma^+$ state in $CO^+$.*

| Vibrational quantum number, v | Binding Energy (eV) | Line Width (FWHM) (eV) | Relative Intensity |
|---|---|---|---|
| 0 | 19,671 | 0,066 | 1,00 |
| 1 | 19,879 | 0,066 | 0,41 |
| 2 | 20,080 | 0,066 | 0,10 |
| 3 | 20,275 | 0,066 | 0,021 |
| 4 | 20,462 | 0,066 | 0,004 |
| 5 | 20,650 | 0,094 | 0,001 |
| 6 | 20,856 | 0,094 | 0,0004 |
| 7 | 21,055 | 0,082 | 0,0003 |
| 8 | 21,261 | 0,082 | 0,0003 |
| 9 | 21,424 | 0,071 | 0,0002 |
| 10 | 21,593 | 0,071 | 0,0002 |

*Table 13. Vibrational energy levels for the $C^2\Sigma^+$ state in $CO^+$.*

| Vibrational quantum number, v | Binding Energy (eV) | Line Width (FWHM) (eV) | Relative Intensity |
|---|---|---|---|
| 0 | 23,01 | 0,07 | 0,2 |
| 1 | 23,195 | 0,071 | 0,72 |
| 2 | 23,381 | 0,068 | 1,00 |
| 3 | 23,559 | 0,080 | 0,83 |
| 4 | 23,734 | 0,071 | 0,75 |
| 5 | 23,877 | 0,071 | 0,61 |
| 6 | 23,993 | 0,071 | 0,43 |
| 7 | 24,084 | 0,071 | 0,33 |
| 8 | 24,168 | 0,071 | 0,28 |
| 9 | 24,249 | 0,071 | 0,24 |
| 10 | 24,329 | 0,068 | 0,23 |
| 11 | 24,410 | 0,068 | 0,21 |

*Table 14. Vibrational energy levels for the $D^2\Pi$ state in $CO^+$.*

| Vibrational quantum number, v | Binding Energy (eV) | Line Width (FWHM) (eV) | Relative Intensity |
|---|---|---|---|
| 0 | 22,204 | 0,07 | 0,07 |
| 1 | 22,380 | 0,07 | 0,3 |
| 2 | 22,554 | 0,07 | 0,7 |
| 3 | 22,726 | 0,07 | 1,0 |
| 4 | 22,895 | 0,07 | 1,0 |
| 5 | 23,062 | 0,08 | 0,7 |
| 6 | 23,225 | 0,07 | 0,2 |

*Table 15. Vibrational energy levels for the $E^2\Pi$ state in $CO^+$.*

| Vibrational quantum number, v | Binding Energy (eV) | Line Width (FWHM) (eV) | Relative Intensity |
|---|---|---|---|
| 0 | 24,755 | 0,09 | 0,6 |
| 1 | 24,937 | 0,08 | 0,7 |
| 2 | 25,115 | 0,08 | 0,9 |
| 3 | 25,294 | 0,08 | 1,0 |
| 4 | 25,484 | 0,08 | 0,9 |
| 5 | 25,658 | 0,07 | 0,8 |
| 6 | 25,836 | 0,09 | 0,6 |
| 7 | 26,000 | 0,08 | 0,4 |

*Table 16. Vibrational energy levels for the $F^2\Sigma^+$ state in $CO^+$.*

| Vibrational quantum number, v | Binding Energy (eV) | Line Width (FWHM) (eV) | Relative Intensity |
|---|---|---|---|
| 0 | 27,876 | 0,08 | 0,6 |
| 1 | 28,063 | 0,1 | 1,0 |
| 2 | 28,240 | 0,09 | 1,0 |
| 3 | 28,400 | 0,09 | 0,7 |
| 4 | 28,582 | 0,09 | 0,4 |
| 5 | 28,768 | 0,07 | 0,2 |

*Table 17. Vibrational energy levels for the $K^2\Sigma^+$ state in $CO^+$.*

| Vibrational quantum number, v | Binding Energy (eV) | Line Width (FWHM) (eV) | Relative Intensity |
|---|---|---|---|
| 0 | 32,814 | 0,071 | 0,93 |
| 1 | 32,984 | 0,078 | 1,00 |
| 2 | 33,162 | 0,085 | 0,77 |
| 3 | 33,323 | 0,12 | 0,31 |

*Table 18. Summary of the observed states in $O_2^+$.*

| State Designation | Adiabatic Ionization Energy (eV) | Vertical Ionization Energy (eV) |
|---|---|---|
| $X\ ^2\Pi_g$ | 12,074 | 12,307 |
| $a\ ^4\Pi_u$ | 16,087 | 16,687 |
| $A\ ^2\Pi_u$ | 17,180 [a] | |
| $b\ ^4\Sigma_g^-$ | 18,171 | 18,171 |
| $B\ ^2\Sigma_u^-$ | 20,321 | 20,458 |
| $^2\Pi_u$ | - | 23,9 |
| $c\ ^4\Sigma_u^-$ | 24,777 | 24,777 |
| $^2\Sigma_u^-$ | - | 27,3 |

a Value given by Huber and Herzberg [18].

*Table 19. Vibrational energy levels for the $X^2\Pi_g$ state in $O_2^+$.*

| Vibrational quantum number, v | Binding Energy (eV) | Line Width (FWHM) (eV) | Relative Intensity |
|---|---|---|---|
| 0 | 12,074 | 0,078 | 0,50 |
| 1 | 12,307 | 0,078 | 1,00 |
| 2 | 12,534 | 0,078 | 0,80 |
| 3 | 12,757 | 0,078 | 0,33 |
| 4 | 12,978 | 0,078 | 0,086 |
| 5 | 13,194 | 0,080 | 0,015 |
| 6 | 13,413 | 0,11 | 0,0015 |
| 7 | 13,624 | 0,089 | 0,0011 |
| 8 | 13,838 | 0,082 | 0,0006 |
| 9 | 14,020 | 0,059 | 0,0007 |

*Table 20. Vibrational energy levels for the $a^4\Pi_u$ state in $O_2^+$.*

| Vibrational quantum number, v | Binding Energy (eV) | Line Width (FWHM) (eV) | Relative Intensity |
|---|---|---|---|
| 0 | 16,087 | 0,073 | 0,07 |
| 1 | 16,211 | 0,073 | 0,26 |
| 2 | 16,335 | 0,073 | 0,53 |
| 3 | 16,455 | 0,075 | 0,77 |
| 4 | 16,574 | 0,075 | 0,95 |
| 5 | 16,687 | 0,073 | 1,00 |
| 6 | 16,801 | 0,073 | 0,92 |
| 7 | 16,911 | 0,073 | 0,81 |
| 8 | 17,017 | 0,073 | 0,66 |
| 9 | 17,122 | 0,073 | 0,53 |
| 10 | 17,225 | 0,075 | 0,41 |
| 11 | 17,326 | 0,075 | 0,32 |
| 12 | 17,425 | 0,075 | 0,27 |
| 13 | 17,521 | 0,080 | 0,24 |
| 14 | 17,616 | 0,078 | 0,20 |
| 15 | 17,703 | 0,078 | 0,18 |
| 16 | 17,791 | 0,078 | 0,16 |
| 17 | 17,874 | 0,078 | 0,14 |
| 18 | 17,954 | 0,078 | 0,13 |
| 19 | 18,034 | 0,080 | 0,12 |

*Table 21. Vibrational energy levels for the $A^2\Pi_u$ state in $O_2^+$.*

| Vibrational quantum number, v | Binding Energy (eV) | Line Width (FWHM) (eV) | Relative Intensity |
|---|---|---|---|
| a | 18,155 | 0,073 | 1,00 |
| | 18,299 | 0,073 | 0,80 |
| | 18,439 | 0,073 | 0,38 |
| | 18,573 | 0,073 | 0,15 |
| | 18,704 | 0,078 | 0,057 |
| | 18,828 | 0,087 | 0,021 |
| | 18,938 | 0,089 | 0,007 |
| | 19,048 | 0,059 | 0,001 |
| | 19,175 | 0,035 | 0,001 |

a Uncertain vibrational quantum number designation.

*Table 22. Vibrational energy levels for the $b^4\Sigma_g^-$ state in $O_2^+$.*

| Vibrational quantum number, v | Binding Energy (eV) | Line Width (FWHM) (eV) | Relative Intensity |
|---|---|---|---|
| 0 | 18,171 | 0,068 | 1,00 |
| 1 | 18,314 | 0,068 | 0,80 |
| 2 | 18,454 | 0,068 | 0,37 |
| 3 | 18,589 | 0,068 | 0,13 |
| 4 | 18,719 | 0,068 | 0,05 |
| 5 | 18,844 | 0,075 | 0,02 |

*Table 23. Vibrational energy levels for the $B^2\Sigma_u^-$ state in $O_2^+$.*

| Vibrational quantum number, v | Binding Energy (eV) | Line Width (FWHM) (eV) | Relative Intensity |
|---|---|---|---|
| 0 | 20,321 | 0,073 | 0,84 |
| 1 | 20,458 | 0,073 | 1,00 |
| 2 | 20,588 | 0,071 | 0,70 |
| 3 | 20,715 | 0,071 | 0,38 |
| 4 | 20,837 | 0,071 | 0,18 |
| 5 | 20,953 | 0,071 | 0,079 |
| 6 | 21,065 | 0,071 | 0,034 |
| 7 | 21,171 | 0,075 | 0,015 |
| 8 | 21,274 | 0,08 | 0,008 |
| 9 | 21,373 | 0,08 | 0,005 |
| 10 | 21,458 | 0,07 | 0,003 |
| 11 | 21,539 | 0,07 | 0,002 |
| 12 | 21,630 | 0,07 | 0,001 |
| 13 | 21,715 | 0,07 | 0,001 |
| 14 | 21,798 | 0,05 | 0,0005 |
| 15 | 21,850 | 0,05 | 0,0006 |
| 16 | 21,910 | 0,05 | 0,0005 |

*Table 24. Vibrational energy levels for the $c^4\Sigma_u^-$ state in $O_2^+$.*

| Vibrational quantum number, v | Binding Energy (eV) | Line Width (FWHM) (eV) | Relative Intensity |
|---|---|---|---|
| 0 | 24,58 [a] | - | - |
| 1 | 24,777 | 0,068 | 1,00 |
| 2 | 24,980 | 0,11 | 0,02 |

a From ref. [9].

## FIGURES

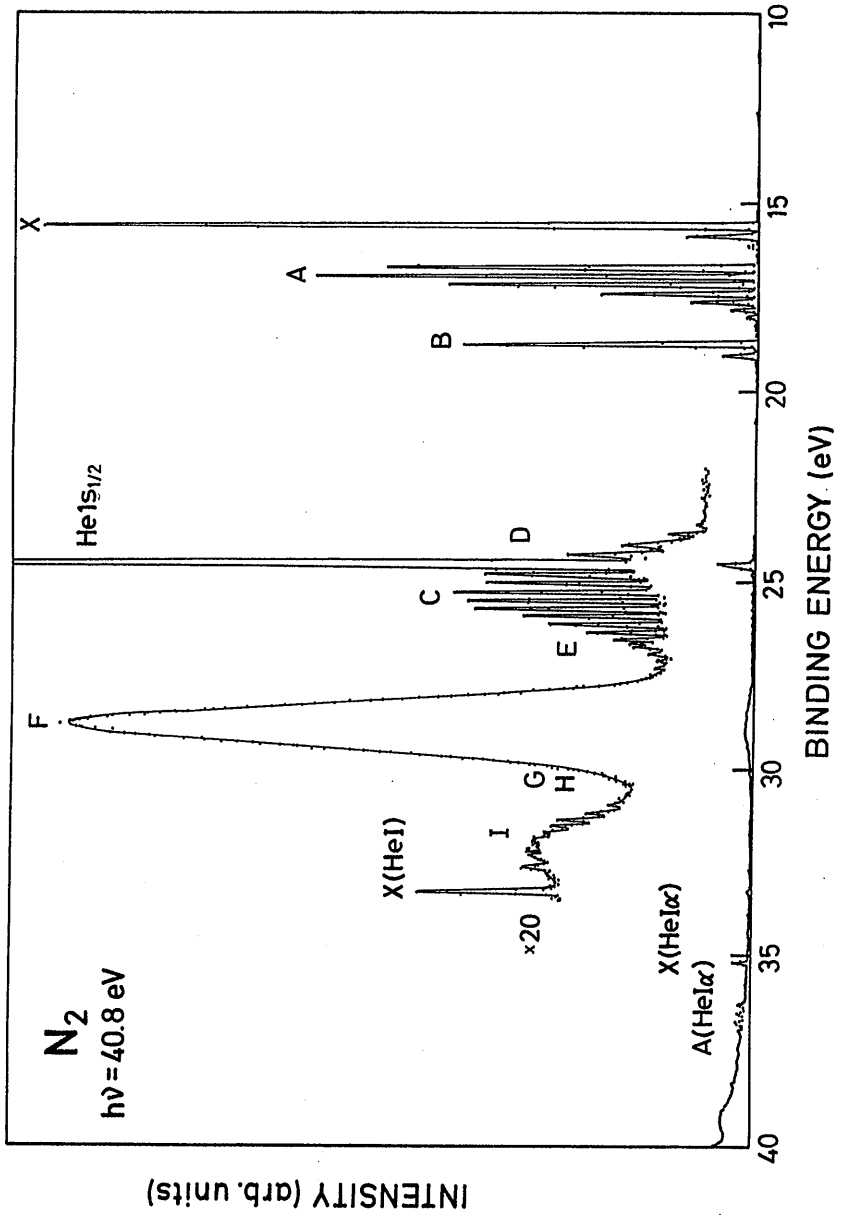


*Fig. 1.* *The valence photoelectron spectrum of $N_2$ excited by monochromatized HeII$\alpha$ radiation.*

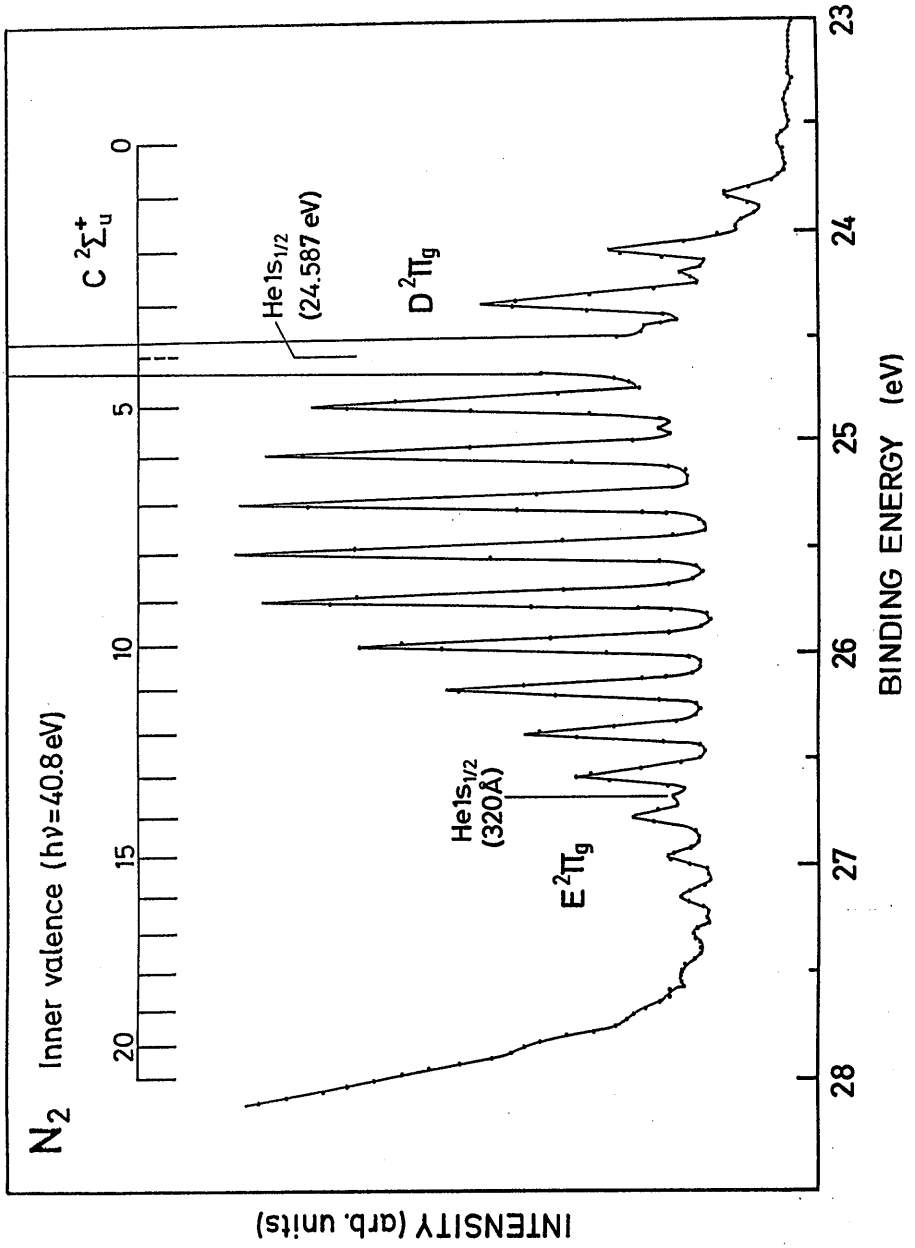


***Fig. 2.*** *A detail of energy region from 23-28 eV of the spectrum shown in Fig.1.*

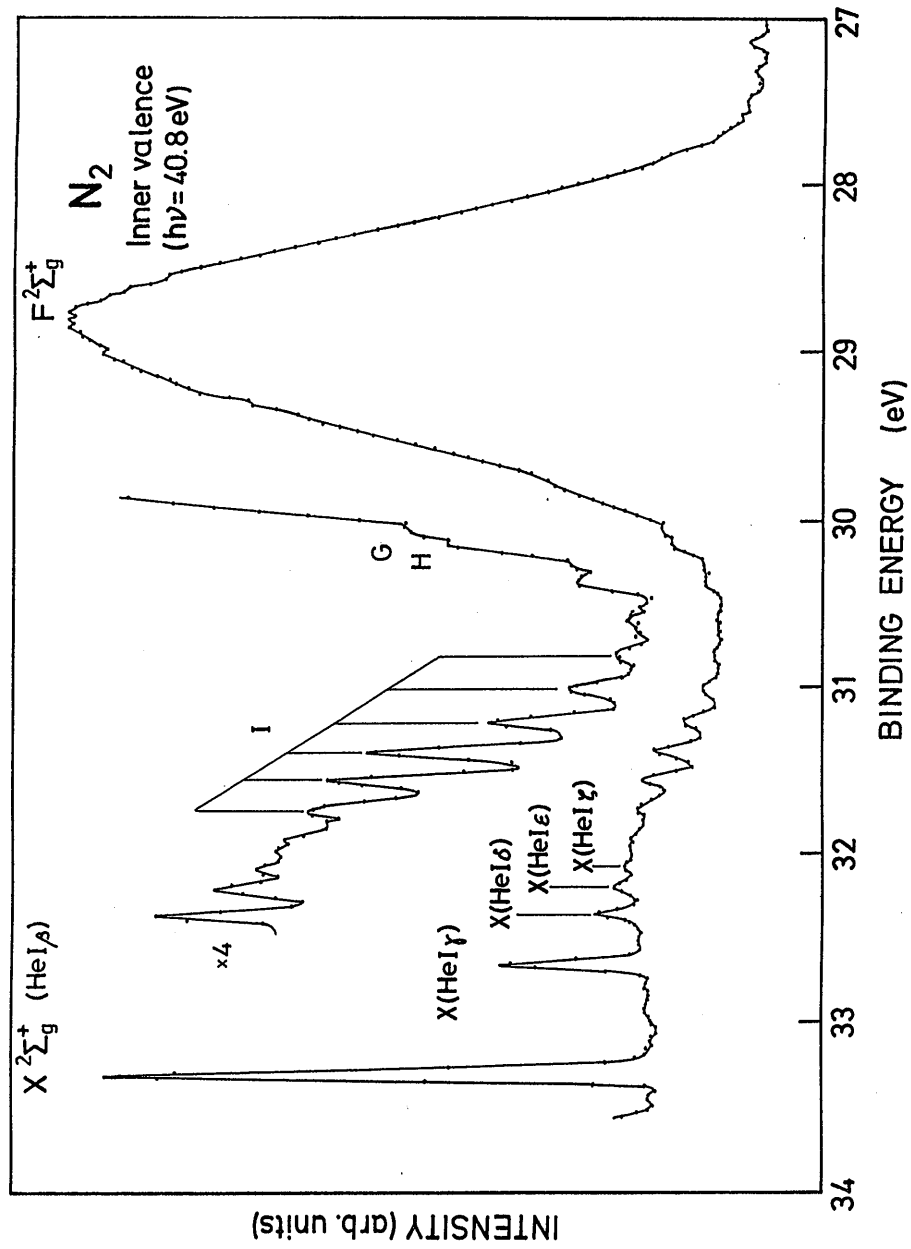


*Fig. 3.* *A detail of energy region from 27-34 eV of the spectrum shown in Fig.1.*

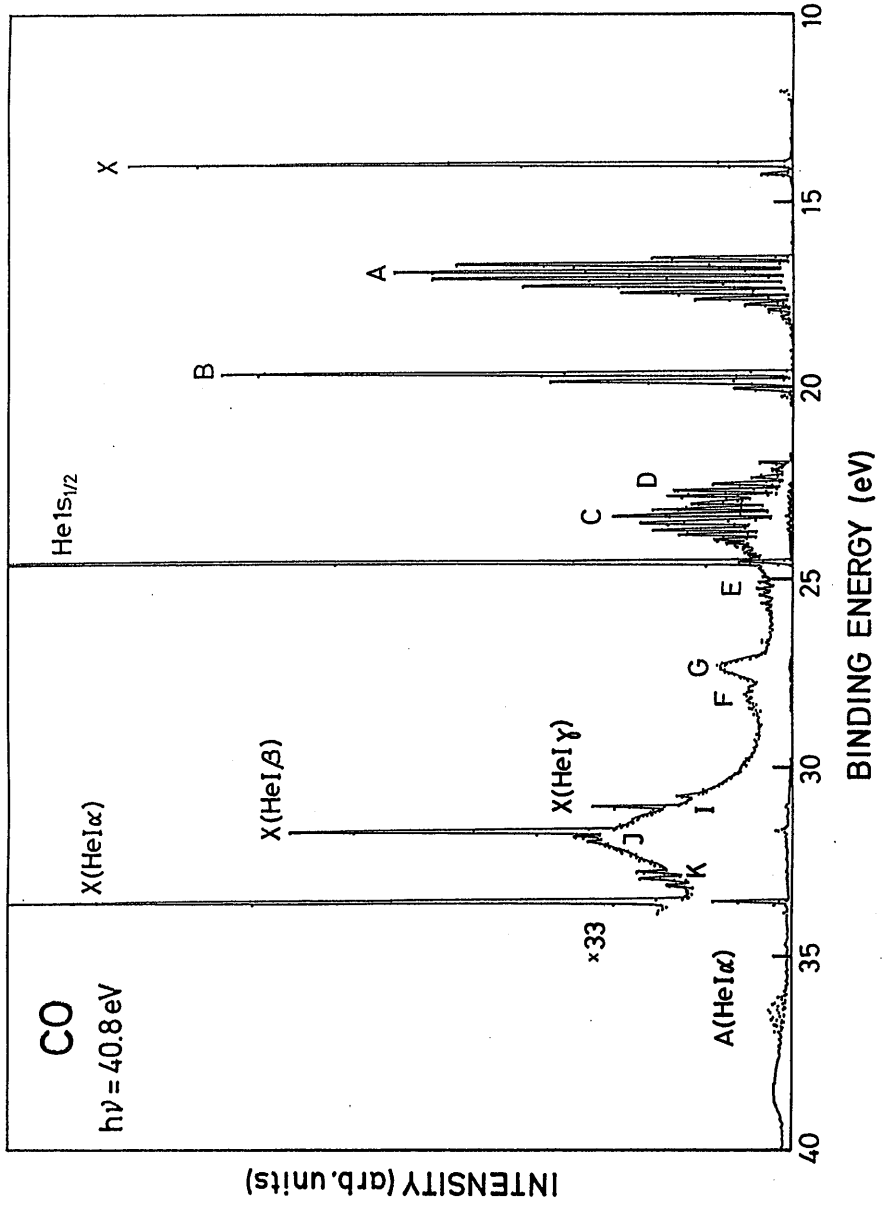


*Fig. 4. The valence photoelectron spectrum of CO excited by monochromatized HeII$\alpha$ radiation.*

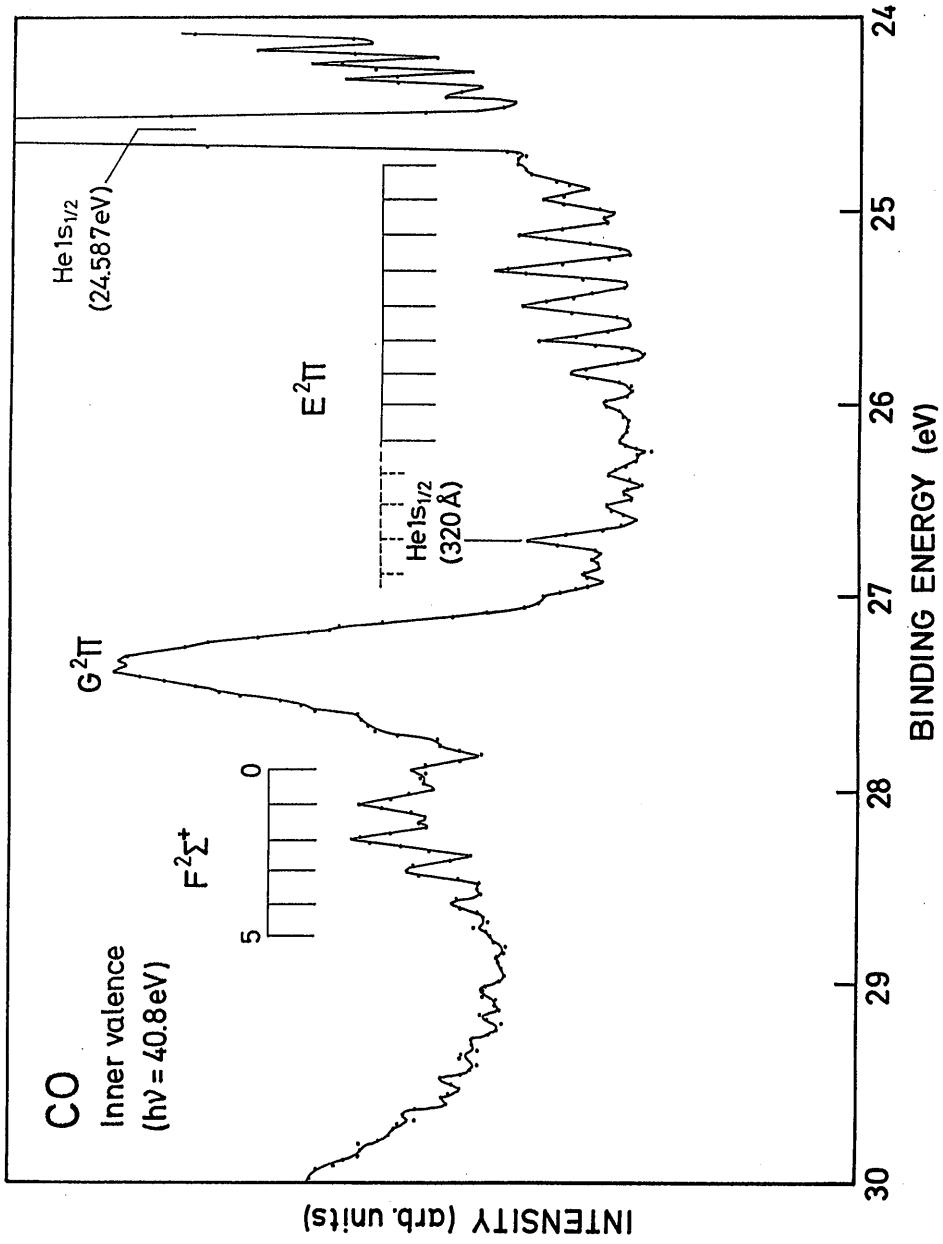


*Fig. 5. A detail of energy region from 24-30 eV of the spectrum shown in Fig.4.*

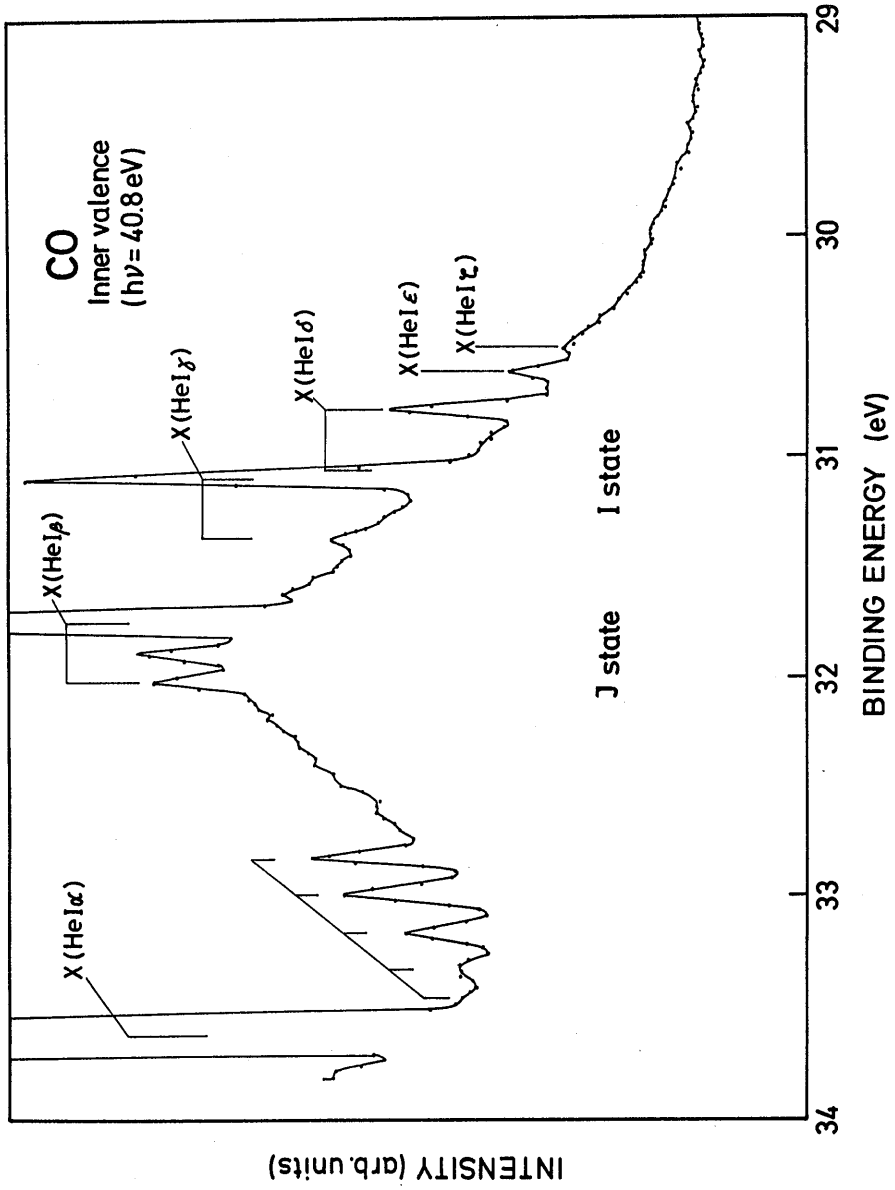


*Fig. 6. A detail of energy region from 29-34 eV of the spectrum shown in Fig.4.*

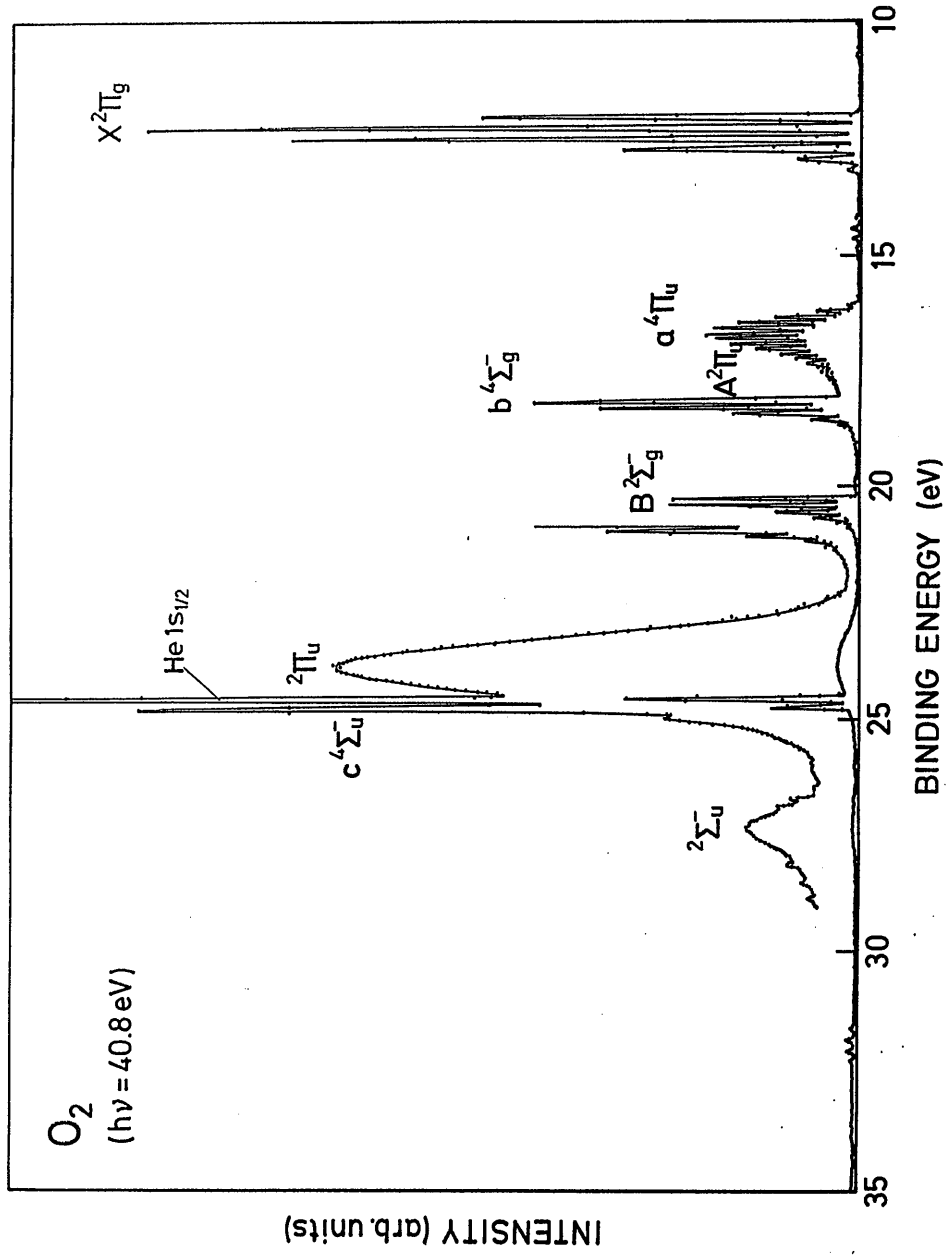


*Fig. 7.* *The valence photoelectron spectrum of $O_2$ excited by monochromatized HeII$\alpha$ radiation.*

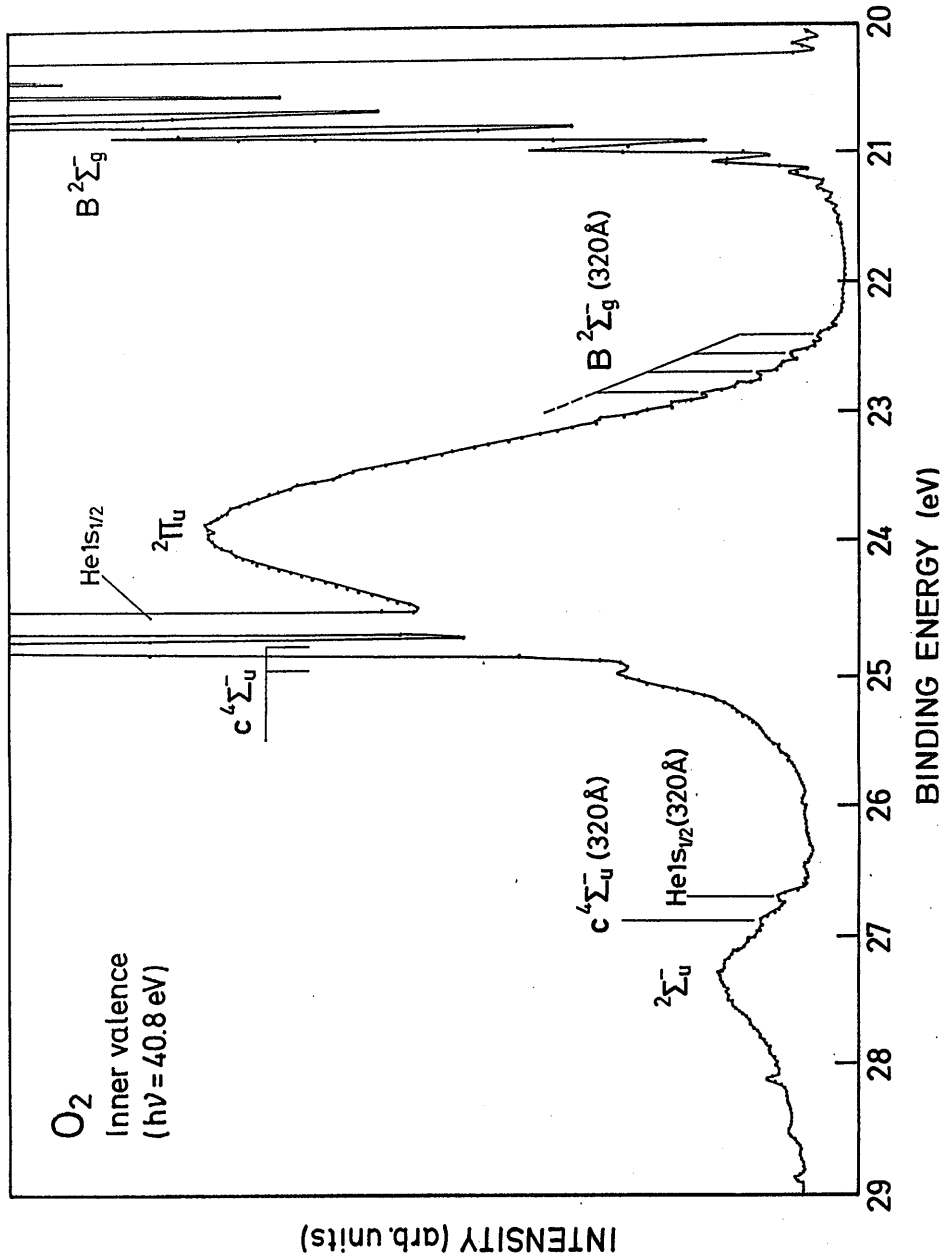


*Fig. 8. A detail of energy region from 20-29 eV of the spectrum shown in Fig.7.*

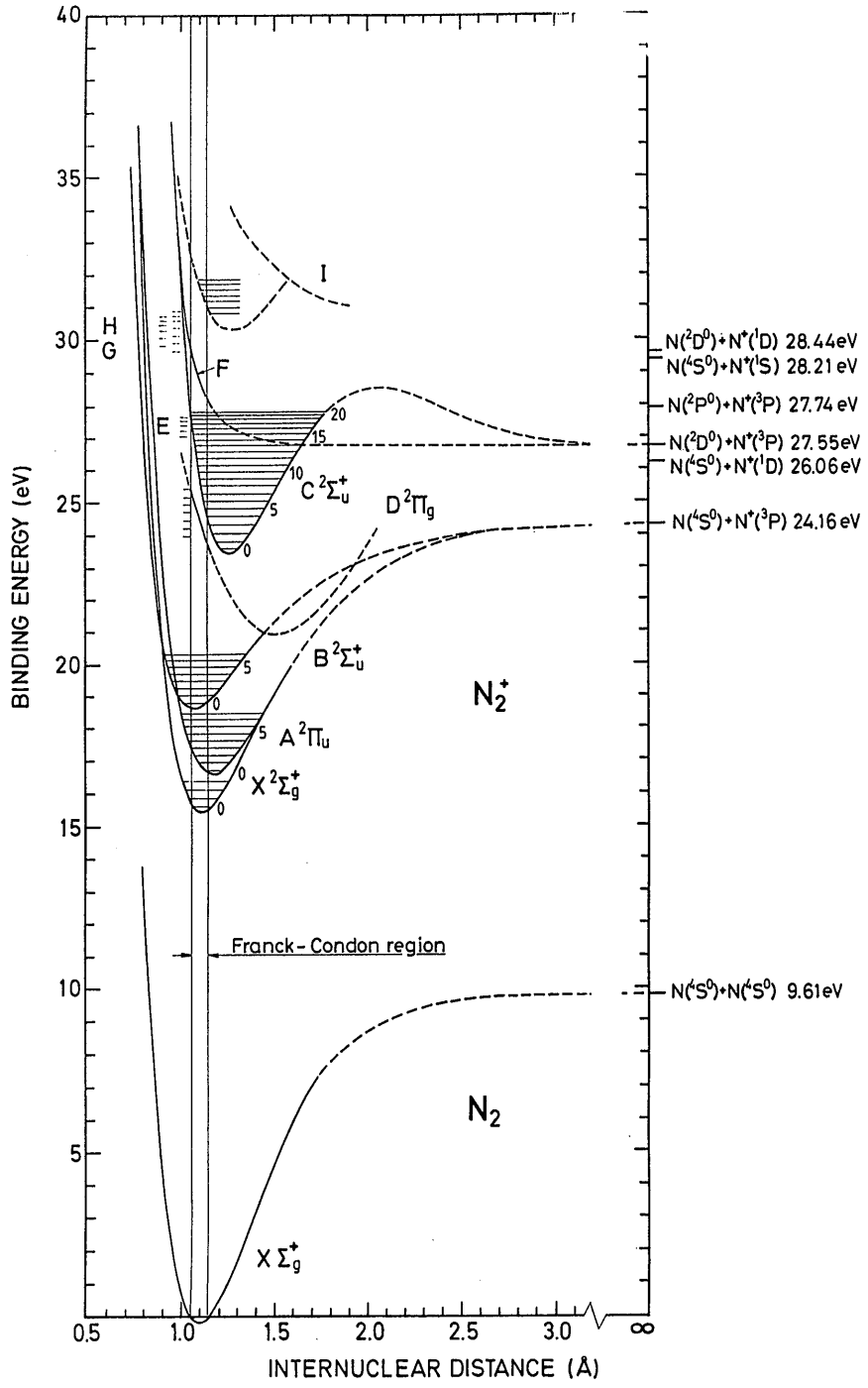


*Fig. 9. The Morse potential curves for $N_2^+$ obtained in this study.*

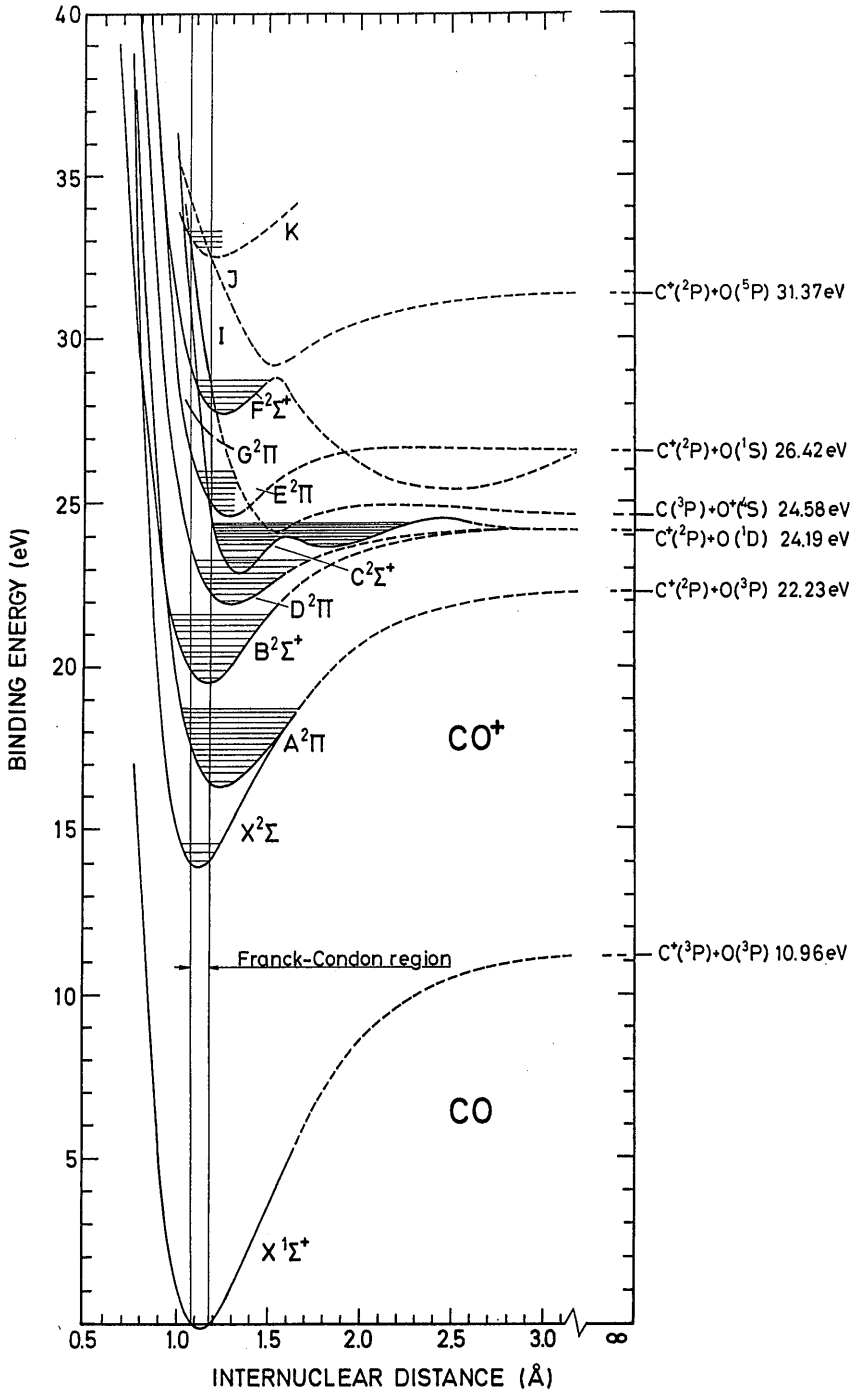


*Fig. 10. The Morse potential curves for $CO^+$ obtained in this study.*

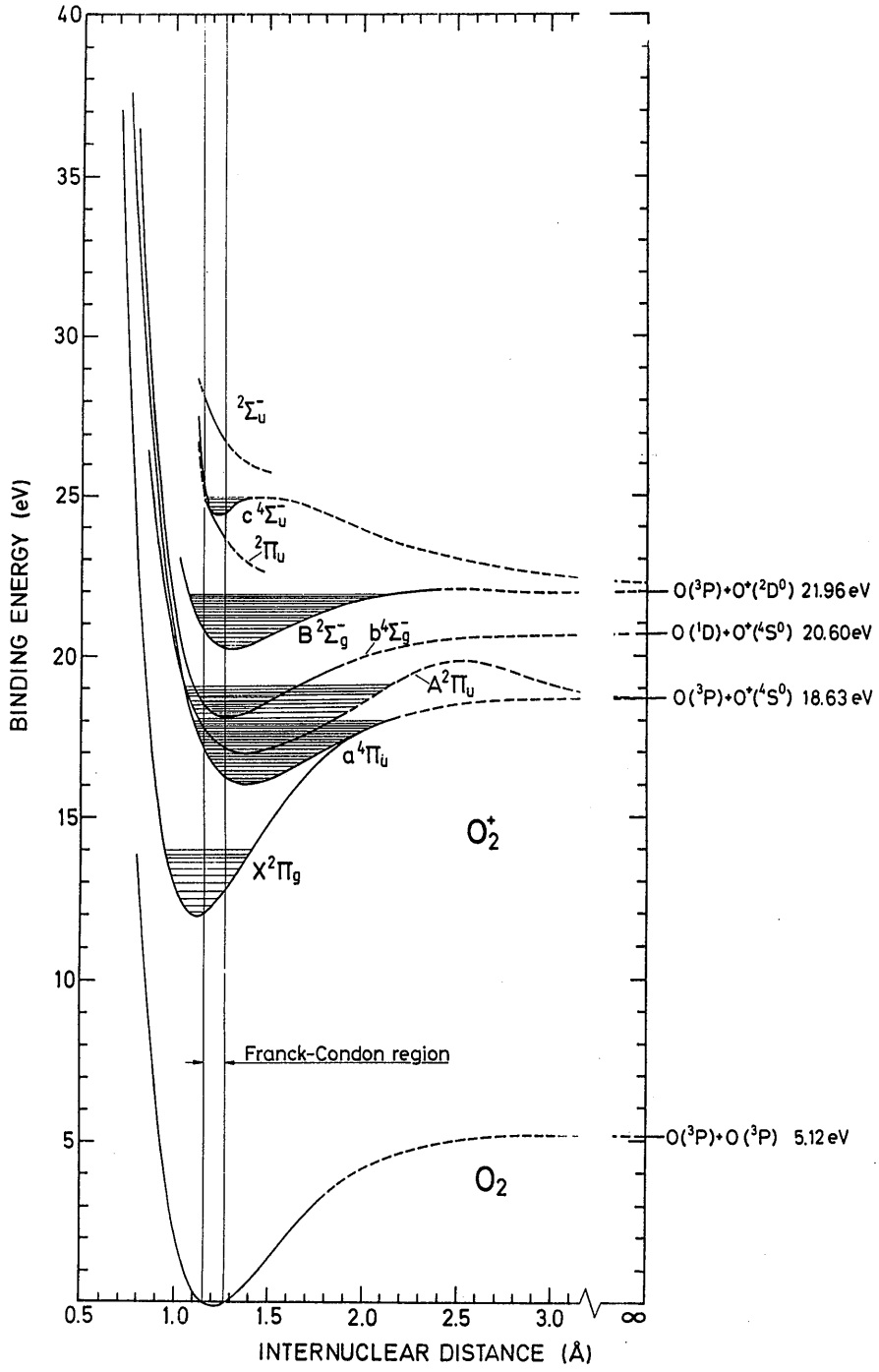


*Fig. 11. The Morse potential curves for $O_2^+$ obtained in this study.*